AD-A152 113 OPTOGALVANIC MEASUREMENT OF EVEN PARITY RYDBERG LEVELS IN KRYPTON GAS(U) AIR FORCE INST OF TECH WRIGHT-PATTERSON AFB OH SCHOOL OF ENGINEERING 1/1

UNCLASSIFIED M S KANDOLA DEC 84 AFIT/GEO/PH/84D-2 F/G 7/4 NL

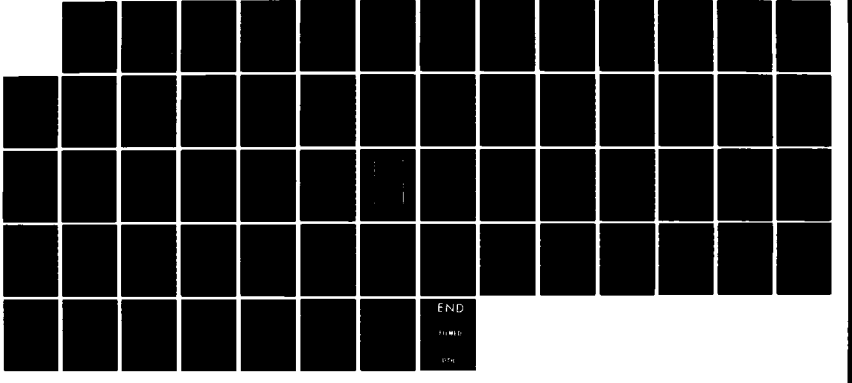

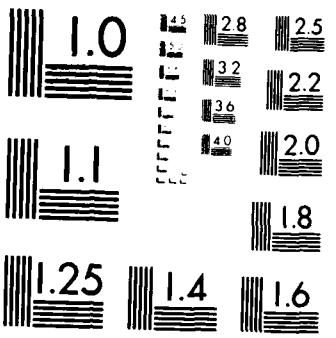

OPTOGALVANIC MEASUREMENT OF EVEN PARITY RYDBERG LEVELS IN KRYPTON GAS

THESIS

Mikal S. Kandola
First Lieutenant, USAF

AFIT/GEO/PH/84D-2

DEPARTMENT OF THE AIR FORCE
AIR UNIVERSITY

AIR FORCE INSTITUTE OF TECHNOLOGY

Wright-Patterson Air Force Base, Ohio

AFIT/GEO/PH/84D-2

OPTOGALVANIC MEASUREMENT OF EVEN PARITY RYDBERG LEVELS IN KRYPTON GAS

THESIS

Mikal S. Kandola
First Lieutenant, USAF

AFIT/GEO/PH/84D-2

AFIT/GEO/PH/84D-2

OPTOGALVANIC MEASUREMENT OF EVEN PARITY RYDBERG LEVELS IN KRYPTON GAS

THESIS

Presented to the Faculty of the School of Engineering

of the Air Force Institute of Technology

Air University

In Partial Fulfillment of the

Requirements for the Degree of

Master of Science

Mikal S. Kandola, B.S.
First Lieutenant, USAF

December 1984

Preface

The objective of this experimental effort was to obtain pressure dependent energy measurements of the even parity Rydberg levels in krypton. Knowledge of these energies and the pressure dependent behavior of the data would provide information important for the development of laser sources.

Unfortunately, the presence of impurities in the krypton-helium mixture used went undetected for too long a period of time at the beginning of the effort. This time delay resulted in having to settle for energy level measurements at a single pressure.

Accurate energy measurements were nonetheless obtained. Thirty different electron transitions were identified, nineteen of which had not been previously reported.

In performing the experiment, I received a great deal of help from several people. I am especially grateful for the assistance I received from my sponsor, Dr. Bish Ganguly. Many thanks are also owed to Mr. Jim Ray from the glass-blowing shop for his patience and cooperation in getting the discharge tube to operate properly. I also wish to thank my advisor, Dr. Roh, for putting up with me and my infrequent visits. Finally, I have to mention my indebtedness to LTC Kussmanoff for his help in getting me through a difficult summer.

Mikal S. Kandola

Table of Contents

Table of Contents

List of Figures

List of Tables

Abstract

An optogalvanic detection scheme, in conjunction with a single-step pulsed laser excitation has been used to measure the energy of even parity Rydberg levels in krypton. The excitation scheme starts from the 5s[3/2]2 and 5s'[1/2]0 metastable states, which have been populated in a He-Kr discharge tube.

Members belonging to the even parity series np[1/2]1, np[5/2]3, np[3/2]1, np[3/2]2, nf[5/2]3, nf[3/2]2, np'[3/2]1, and np'[1/2]1 have been observed and their energies measured with an accuracy of 0.9 cm^{-1}. The 4f'[5/2]2 term was also observed and it has been found to originate from the 5s[3/2]2 metastable level, in violation of selection rules.

Measured energies were compared to either calculated or previously measured values. Calculated energies were determined with the Rydberg formula using quantum defects extrapolated from the known low-lying levels.

OPTOGALVANIC MEASUREMENT OF EVEN PARITY RYDBERG LEVELS IN KRYPTON GAS

I. Introduction

Background

The rare gas atom krypton has thirty-six electrons and is the final entry in the first long period of elements. Like the other rare gases, its outer shell is completely filled with electrons. Consequently, the normal state of krypton is $^1S_0$. That is, the quantum numbers J, L, and s are all zero. When one of the six electrons in the outer 4p shell is excited to a higher energy level, the state or term value of the atom core is changed. The new state, determined from the remaining five p electrons, is ^2P_J and J is either 1/2 or 3/2. The excited electron may take on a value of n greater than or equal to four for d and f states, and five for s and p states. Known energies of these excited states are shown in the energy level diagram of Figure 1.

A continuing effort is being made by researchers to obtain measurements of the higher energy levels. Since the compilation of krypton energies by the National Bureau of Standards in 1952, and Humphreys and Kaufman in 1969, the progress in the field can be summarized by four recent papers:

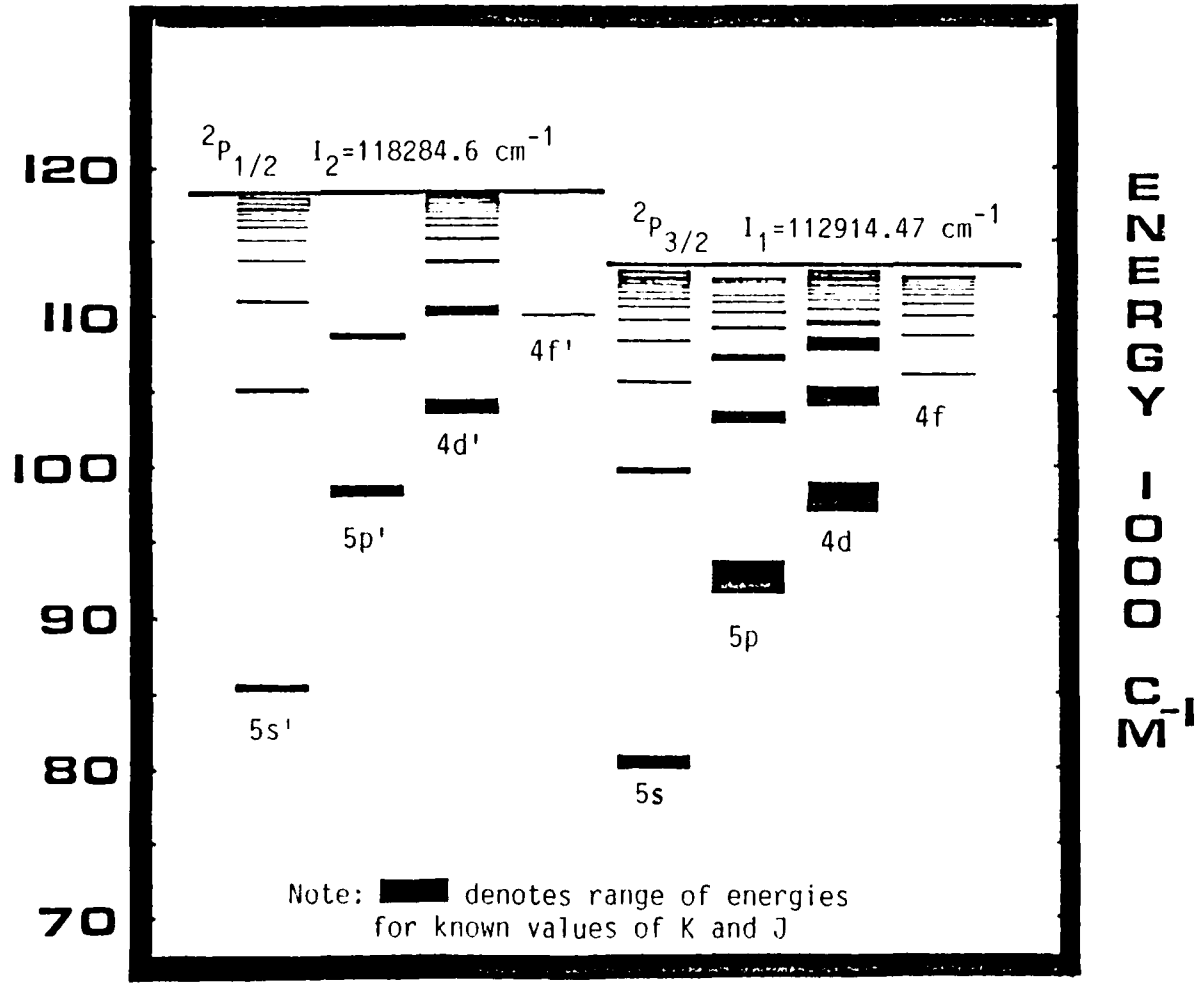

Figure 1. Energy Level Diagram of Known Krypton Levels

(i) a study of the even high-lying np' and nf' levels using photoionisation detection of krypton metastable atoms in an atomic beam which have been excited with a tunable UV laser (Dunning and Stebbings, 1974);

(ii) a recording of the vacuum uv absorption spectra of the ns[3/2]1, ns'[1/2]1, nd[1/2]1, nd[3/2]1, and the nd'[3/2]1 Rydberg series (Tanaka and Yoshino, 1979);

(iii) a two-step laser excitation investigation of seven odd ns and nd Rydberg levels from a beam of krypton metastable atoms using the field ionisation detection method (Delsart and others, 1981:4241-4254);

(iv) a two-step laser excitation investigation of both the odd nd[3/2]2 and nd[7/2]3, and even np[5/2]3, nf[7/2]J, and nf[9/2]J Rydberg levels using a helium-krypton discharge and optogalvanic detection (Delsart and others, 1981:3355-3361).

Various types of spectroscopic techniques have been used to obtain the energy levels of the excited atom. The most recent additions to the list of energy levels have been determined using the optogalvanic technique. The optogalvanic spectroscopic technique used in this work is similar in many respects to the generation of excitation spectra. In the former, however, no optical measurements are required in monitoring the spectra. Consequently, problems associated with scattered excitation light and background light are not a factor in the sensitivity of the measurements (King and Schenck, 1978).

The concept behind optogalvanic spectroscopy has been known for some time. Early work with the effects of radiation on the lifetimes and concentration of metastable atoms was performed in the 1920's

(Meissner and Miller, 1953). Briefly, the optogalvanic effect is based on the fact tnat irradiation of a low-pressure gas discharge tube with monochromatic light will produce a change in the voltage across the tube when the incident light is resonant with a transition occurring in the discharge (Green and others, 1976:727). When the radiation absorbed produces transitions to higher states from which ionization occurs more easily, the discharge voltage will decrease, since the electron temperature required to maintain the ionization rate is decreased (Bridges, 1977:352). This voltage signal is readily detectable with measurement electronic equipment.

In view of the measurements for odd krypton Rydberg levels obtained by Delsart using a two-step optogalvanic process, measurements for the even levels should be possible using a variation of his approach. Considering the extent of known even krypton levels, a contribution to the list would be of interest to the scientific community.

Problem Statement

The objective of this effort is to record and identify even parity krypton Rydberg series terms approaching the first and second ionisation limits which are at 112914.47 and 118284 cm^{-1} above ground level, respectively. The energies of all observed terms will be determined. The spectrum scan will begin at approximately 110000 and 115200 cm^{-1} for series approaching the first and second ionisation limits, respectively. Starting the scan at these levels will provide measurements overlapping the highest known np series terms.

Approach

Measurement of the even parity krypton spectra will be made using a single-step optogalvanic spectroscopic technique. Krypton metastable atoms of odd parity, created in a low-pressure discharge, will be excited to high-lying even parity states when pumped by the frequency doubled output of a tunable dye laser. The krypton spectra will be recorded simultaneously with that from a neon calibration lamp to provide energy reference points througnout the scan in order to determine the energies of the unknown levels.

II. Theory

j-l Coupling

In some atomic systems and electron configurations, certain interactions are larger than others; whereas in other atomic systems and electron configurations different interactions predominate. The type of vector coupling that is used to model atomic systems consequently depends on what interaction is the strongest.

Two types of coupling generally considered in spectroscopy are the L-S and the j-j coupling schemes. The former takes place when the spin-orbit interaction is weak compared to the electrostatic, the latter when the electrostatic interaction is weaker. Another type of vector coupling, appropriate for the rare gas atoms, is j-l coupling. This type of coupling takes place when the electrostatic interaction is weak compared to the spin-orbit interaction of the parent ion, but is strong compared to the spin coupling of the external electron. In this case, the orbital angular momemtum, l, of the external electron is coupled with the angular momemtum, j, of the ion core yielding an intermediate quantum number K. K is then coupled with the spin of the electron, s, to give a total angular momentum, J (Racah, 1942:537).

Because j-l coupling is intermediate to the L-S and j-j coupling schemes, another notation was needed to accurately describe what was happening physically. An example of this notation for a state in krypton is $(^2P_{3/2})np[3/2]1$. The capital letter in parentheses, P, with its superscript, 2, and subscript, 3/2, represents the parent ion term, its multiplicity, and its total angular momemtum, respectively. The

possible values of j are 1/2 and 3/2 corresponding to terms approaching the first and second ionisation limits, respectively. The letters n and p represent the principal and orbital quantum numbers of the external electron. When the parent term has a j value of 1/2, an apostrophe is used with the orbital quantum number. The half-integral value in square brackets with its integer valued subscript represent K and J, the intermediate and total angular momentum quantum numbers. Possible values of J are given by $J = K \pm 1/2$.

Quantum Defect of Rydberg Atoms

The study of the spectra of highly excited atoms has revealed that the outer electron penetrates less into the core of the atom as the orbital angular momentum becomes larger and that the electron energy states approach those of hydrogen. For an atom with N+1 electrons, the atomic model formed is that of a nucleus surrounded by a core of N electrons outside of which is a single hydrogen-like electron (White, 1934:90).

The quantum defect, u, provides a measure of the penetration into the core and becomes smaller as the electron orbital quantum number, l, gets larger. It also indicates a change in the value of the principal quantum number, n, which yields an effective quantum number n^* where $n^* = n - u$.

The value of the quantum defect can be determined using equation (1), the well-known Rydberg formula (White, 1934:387).

$$I = E + R / (n^*)^2 \qquad (1)$$

I : ionization limit (cm^{-1})

E : energy of electron state (cm^{-1})

R : Rydberg constant (cm^{-1})

R(Kr) = 109736.6

n* : effective quantum number

Analysis of the energies and quantum defects of krypton indicates that, in general, a linear relationship exists between these two parameters in the form

$$u = u_0 + \alpha(E - E_0) \qquad (2)$$

u : quantum defect for energy E

u_0 : quantum defect at reference energy E_0

α : slope of u versus E

E_0 : energy level associated with u_0 (cm^{-1})

E : energy level for which u is desired (cm^{-1})

A plot of the quantum defect versus energy is shown in Figure 2 for the np[3/2], np[3/2]1, and np[5/2]3 series using known energy levels in krypton. Knowledge of the quantum defects for two or more energy levels in a series for small values of principal quantum number n thus allows the slope to be calculated. Using this slope, α , the energies for levels with higher values of n in the series can be calculated. In the case of one-electron atoms, semi-classical considerations have shown that the quantum defect must be an increasing

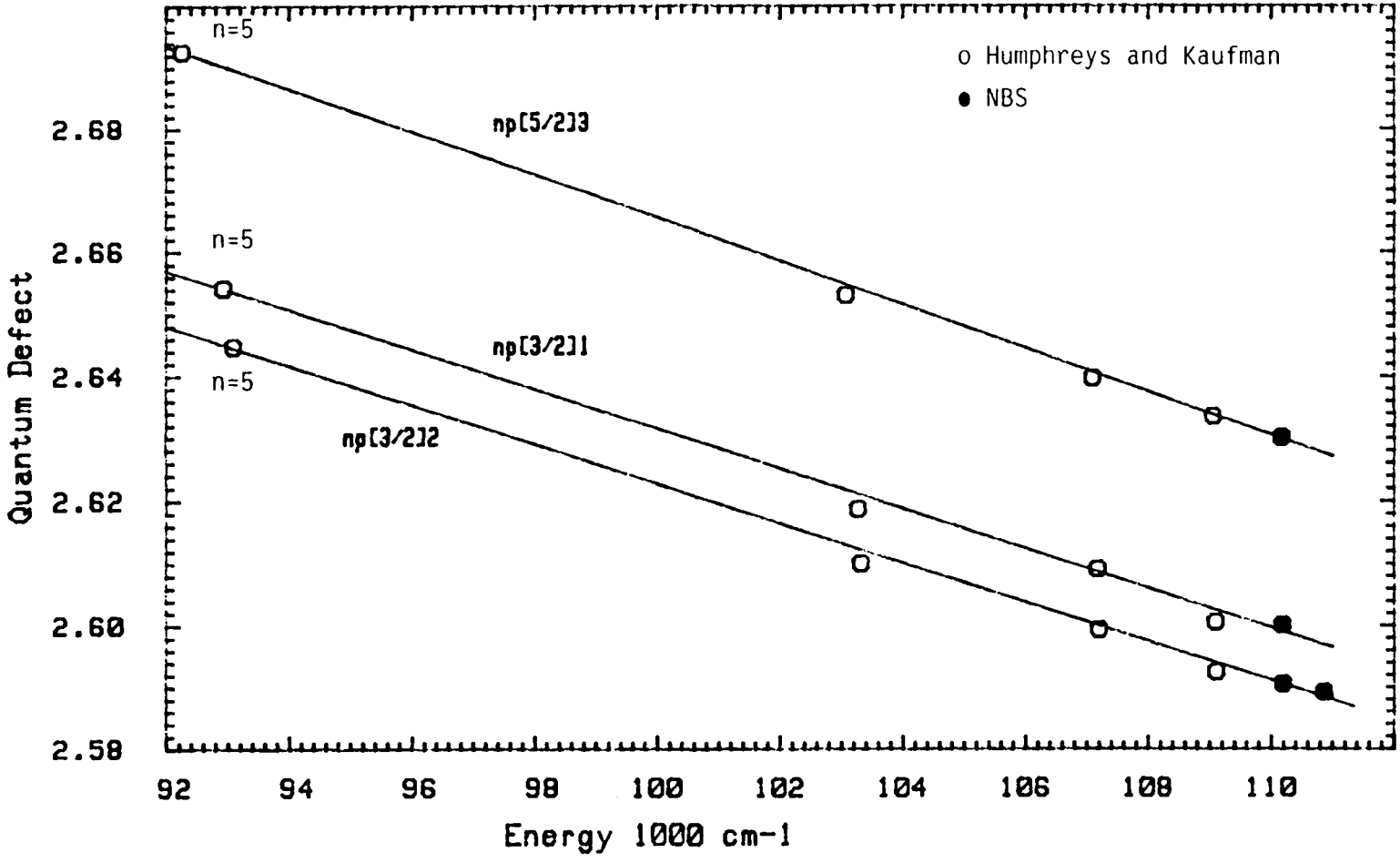

Figure 2. Plot of Quantum Defect vs. Energy for Krypton np[3/2]2, np[3/2]1, and np[5/2]3 Series

function of energy for states that do not penetrate much into the core, e.g., f states, and a decreasing function of energy for penetrating states, e.g., p states (Biraben and others, 1982:2601). This relationship can be seen in Figures 2 and 3. A point that must be considered in calculating energy levels is that of possible perturbations caused by the interaction of different energy levels. Perturbations are treated in the next section. Perturbations can affect energy levels and the intensity of transitions. Figure 3 shows a plot of quantum defect versus energy for the nf[5/2]3 and nf[3/2]2 krypton series for known levels. Some perturbation effect is seen to cause a departure from the linear relationship previously mentioned. These perturbations add some uncertainty to the calculation of higher energy levels when they are not accounted for.

Perturbations

The nature of perturbation between two levels can be thought of basically as a repulsion. The magnitude of this effect increases as the difference in energy between the levels decreases (White, 1934:390). Two levels will perturb each other when both levels have the same parity, and when both levels have the same J value. These levels may belong to the same or different electron configurations. In krypton, perturbations are found to occur between series of the same parity and J value that approach different ionisation limits, for example between p-p', and f-f' levels (Dunning and Stebbings, 1974).

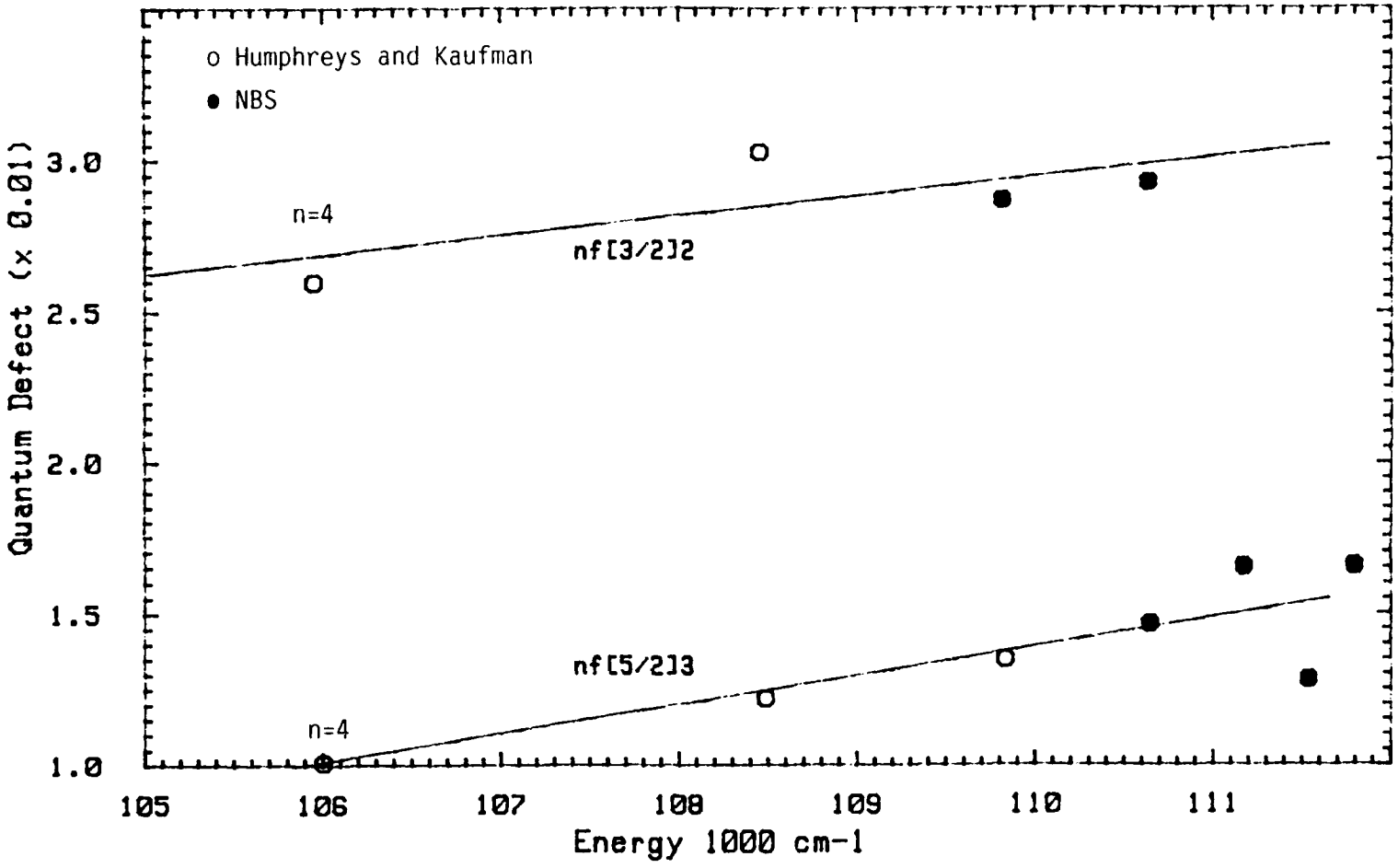

Figure 3. Plot of Quantum Defect vs. Energy for Krypton nf[5/2]3 and nf[3/2]2 Series

Selection Rules and Relative Line Intensities

Regardless of the type of vector coupling used to describe an atomic species, certain general selection rules must hold if an electron transition is to be allowed. For j-l coupling, the selection rules are: $\Delta j = 0$, $\Delta K = 0, \pm 1$, $\Delta J = 0, \pm 1$, where the J = 0 to 0 transition is forbidden. Transitions must also involve a change in parity, e.g., odd to even or even to odd (Faust and McFarlane, 1942:2011).

From an approximation in the analysis of the spectra of the rare gases, it is found that all levels should be doubly degenerate, that two levels with the same value for K but different values of J have approximately the same energy (Shortley and Fried, 1938:749). This pair structure of levels with different J values have all the characteristic properties of doublets, including those for line intensities (Racah, 1942:537). General observations of line intensities for doublet spectra indicate that the strongest lines correspond to electron transitions for which l and J change in the same way. When there exist more than one line for which this is the case, the transitions involving the larger values of J are strongest (White, 1934:118).

These general observations have been verified numerically for relative line strengths between various excited levels of Neon, Argon, Krypton, and Xenon under the assumption of the j-l coupling scheme, using the method of Koster and Statz (Faust and McFarlane, 1964:2011). The relative line strengths obtained for s-p and s'-p' electron transitions are tabulated in Tables I and II, respectively. These relative line strengths are appropriate for optogalvanic spectra when they are used to compare adjacent energy levels for which the energy

LOWER LEVEL	UPPER LEVEL					
	p[1/2]0	p[1/2]1	p[3/2]1	p[3/2]2	p[5/2]2	p[5/2]3
s[3/2]1	2	1	5	1	9	F
s[3/2]2	F	5	1	9	1	14
NOTE: F DENOTES A FORBIDDEN TRANSITION						

Table I. Relative Intensities for s-p Electron Transitions

LOWER LEVEL	UPPER LEVEL			
	p'[1/2]0	p'[1/2]1	p'[3/2]1	p'[3/2]2
s'[1/2]0	F	2	4	F
s'[1/2]1	2	4	2	10
NOTE: F DENOTES A FORBIDDEN TRANSITION				

Table II. Relative Intensities for s'-p' Electron Transitions

separation is very small. In the present case, the difference in wavelengths for pumping to those levels is on the order of 10 angstroms. The absorption cross section of the metastable atoms is then approximately the same for these closely separated pumping wavelengths. The probabilities for the various transitions are calculated by building up a wave function for the rare gas in question (j-l coupling) using Clebsch-Gordon or 3-j coefficients, and evaluating matrix elements of an electric dipole operator between the two desired states (Koster and Statz, 1961:2054).

III. Experimental Procedure and Equipment

System Description and Operation

A block diagram of the experimental setup is shown in Figure 4. A list of all equipment used in the experiment is provided in Appendix A. The Nd:Yag laser is operated at a pulse rate of 10 Hz. The dye laser, working with DCM dye (6030-6820 angstroms) is scanned at a rate of 0.1 angstrom/second. The scan was initiated at a visible wavelength of 6615 angstroms which allows observation of the first neon calibration line at 6598 angstroms. At least seven other neon calibration lines are expected to be observed. These lines are at wavelengths of 6532, 6506, 6402, 6382, 6334, 6304, and 6266 angstroms.

The first krypton line expected is known to lie at an energy above the 5s[3/2]2 metastable level that corresponds to a transition of 3310 angstroms (6620 angstroms for the dye laser). A prism is used to spatially separate the visible and uv outputs from the autotracker. Using a mirror, the visible and uv beams are focused into the neon calibration lamp and through the positive column of the discharge tube, respectively. Because of a drift in spatial positioning with the wavelength scan, these beams had to be checked periodically. The AC component of the discharge tube voltage was coupled to the oscilloscope and to the boxcar through a 2 nF blocking capacitor and bandpass filter.

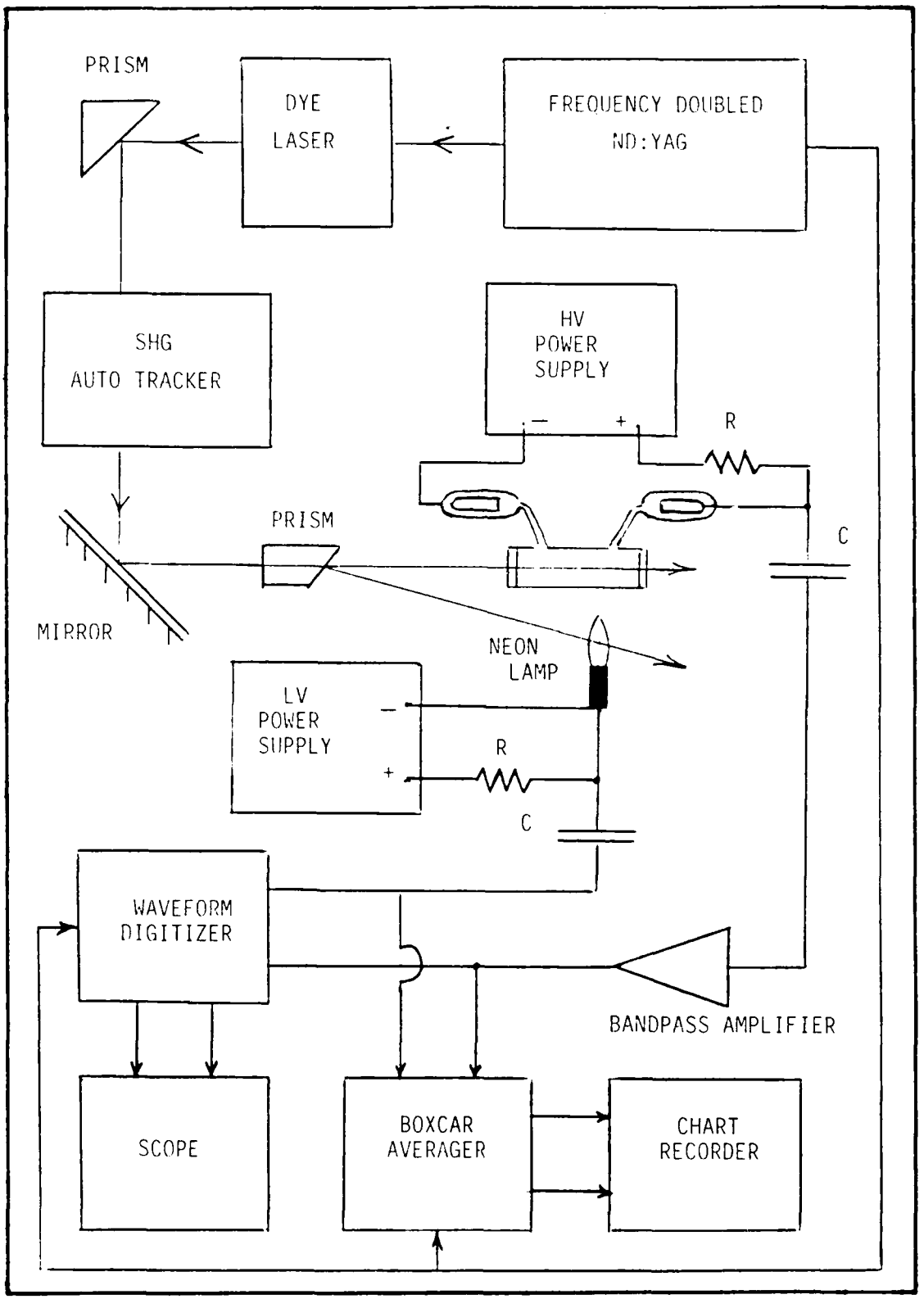

Figure 4. Experimental Equipment Setup

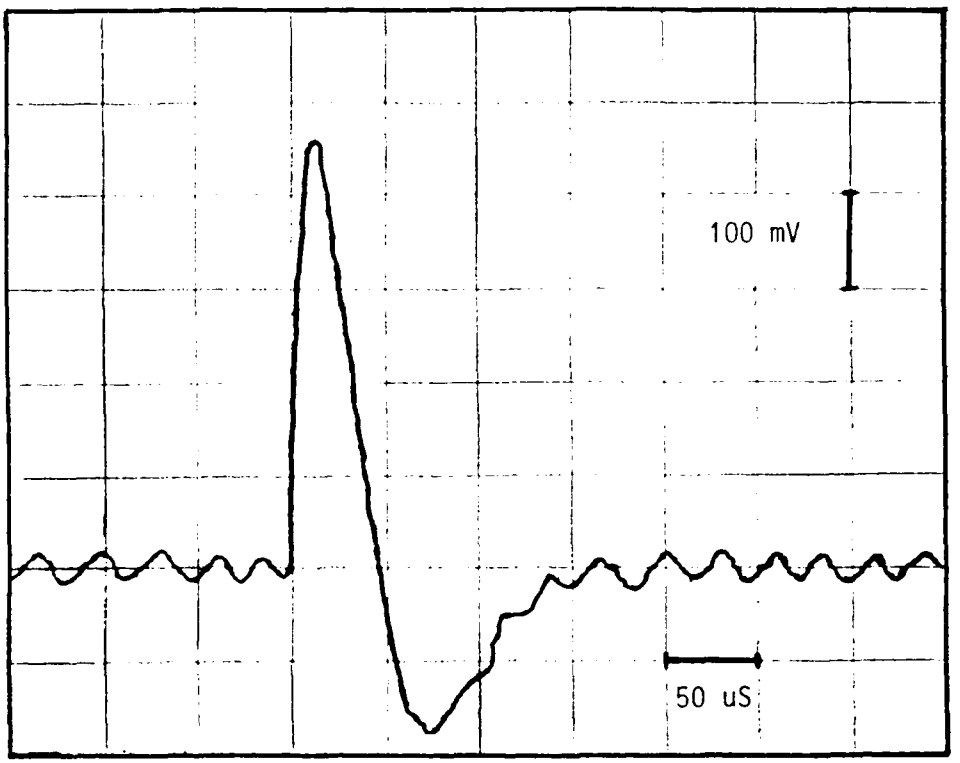

Figure 5. Optogalvanic Response from Discharge Tube

When the incident uv light is resonant with a krypton transition, the discharge is perturbed and subsequently returns to its steady state after an optogalvanic response such as that shown in Figure 5. It is this signal that is sent to the boxcar integrator. The integrator sampling sequence is triggered by the laser sync pulse which corresponds to the point at which the optogalvanic signal begins to increase out of the noise background in Figure 5.

Laser

The laser system used in the experiment was a Quanta-Ray DCR-2A-10 Nd:Yag laser and frequency doubler. The linewidth is approximately 0.8 cm^{-1} at 1.06 microns. The output of the frequency doubled Nd:Yag was directed into a model PDL-1 Pulsed Dye Laser, also manufactured by Quanta-Ray. Exciton DCM dye was used during the experiment. The dye laser was operated at approximately 4 mjoules/pulse at a wavelength of 6400 angstroms and dropped to approximately 3 mjoules/pulse on the lower end of the scan.

SHG Autotracker

An Inrad 5-12 Second Harmonic Generator with KDP-C crystal and Servo-Driver was used to frequency double the visible dye laser output. A beam sampling assembly senses the uv output and adjusts the phase match angle through a feedback loop to maintain maximum conversion efficiency, which is approximately 15%.

Boxcar Integrator

A Princeton Applied Research model 160 Boxcar Integrator was used to sample and average the optogalvanic signal from the discharge tube. The 100 kohm high impedance input was used. A sync signal from the pulsed laser triggers a time base ramp that initiates the opening of the sampling gate, the aperture time of which was 12.5 microseconds.

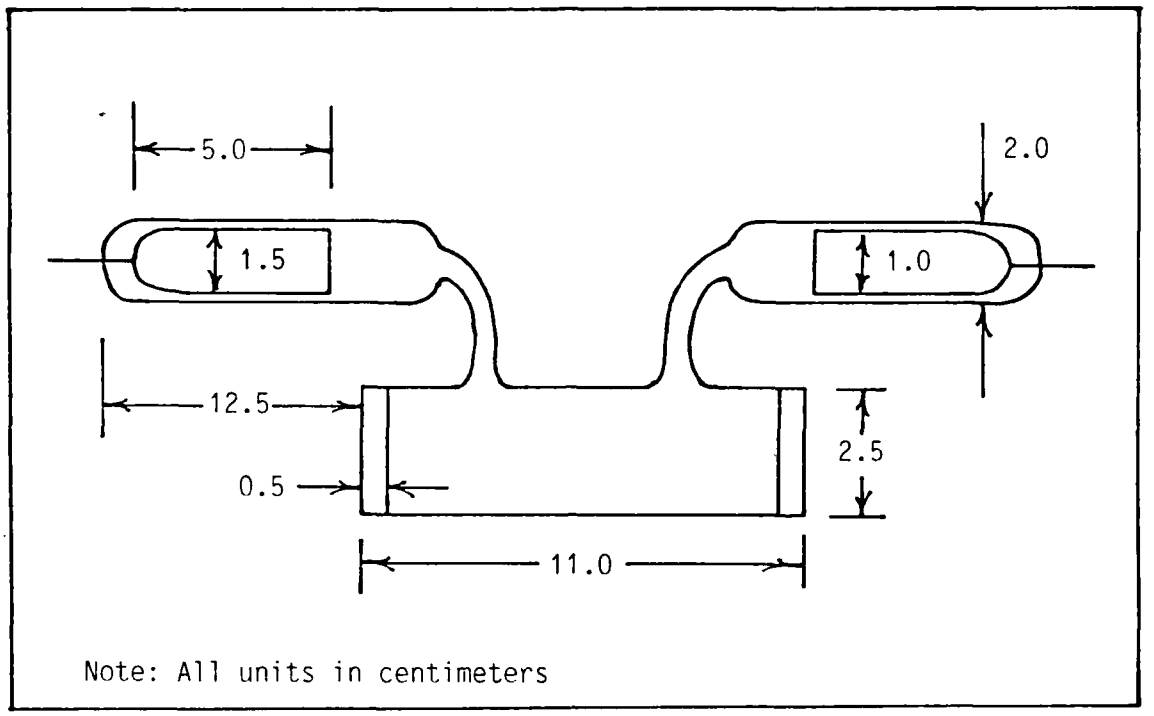

Figure 6. Krypton Discharge Tube

Discharge Tube

A sketch of the discharge tube used in the experiment is shown in Figure 6. A 6% krypton, 94% helium mixture at a total pressure of 1.5 torr was used. Research grade gas was used for both constituents of the mixture. The mixture and pressure chosen were those for which the peak-peak noise voltage appeared minimal. Under these conditions, and with a discharge tube voltage and current of approximately 450 volts (DC) and 0.65 mamps (DC), respectively, the noise voltage was 40 mvolts peak-peak. The voltage applied to the tube was typically 600 volts (DC). A 100 kohm current limiting resistor was used.

IV. Series Identification

Procedure for Calculation of Transition Energies

When the wavelength of the uv light incident upon the discharge tube is resonant with a krypton absorptive transition from a metastable level to a higher level, an optogalvanic signal is produced. The energy of the photon which produces the transition, or the transition energy, corresponds to the energy of a krypton level above that of a metastable level.

Since known and calculated values for krypton energy levels have units of cm^{-1}, the photon or transition energies used to identify the observed transitions will be referred to using these units. These energies are determined with the use of the neon calibration lines. It should be noted that the neon lines correspond to transitions resulting from incident visible light.

The energies of the neon levels above ground are well-known (Adams and others, 1950). The recorded neon transitions are initially identified according to their wavelengths which were read from the dye laser wavelength scale and written onto the scan recording. Once identified, the energies of the neon lines are used to determine the scaling factors. The scale between successive neon levels, cm^{-1} per division, was determined by taking the quotient of energy difference and the separation of the peak positions. The value of this scale factor for the visible is then doubled to obtain a uv scale factor.

The energy separation between a particular krypton transition and a calibration line was obtained by multiplying the appropriate uv scale factor by the distance between the calibration line and the krypton line peak positions. The energy separation is then either added to or subtracted from the uv energy of the calibration line used. It is added when the krypton line appears on the uv side of the calibration line. The uv energy is equal to twice the energy of the neon line. An offset of half a division corresponding to the pen separation had to be taken into account when determining the distance between krypton and neon lines.

Identification of Series Terms

In order to determine the actual energy levels of the observed lines, the energy of the metastable level from which the electron transition occurs must be known. There are two metastable levels to consider; namely, the 5s[3/2]2 and 5s'[1/2]0 levels (Delsart and others, 1981:4242). The energies of these two levels are 79971.8 and 85191.6754 cm^{-1}, respectively (Humphreys and Kaufman, 1969:1618).

Since the probability of transition from a state is proportional to the statistical weight, $g = 2J + 1$, of that state, transitions from the 5s[3/2]2 level are expected to occur more often (Herzberg, 1937:160). Nonetheless, both levels are considered. Two sets of energies for each of the observed series are thus calculated by adding the transition energies to those of the metastable levels.

Candidate series for the observed lines are determined using the selection rules for j-l coupling. Initial identification of the candidate series terms can then be made by comparing the measured data

to either known or calculated values. Accurate energy measurements for low-lying even parity krypton levels have been made by Humphreys and Kaufman (Humphreys and Kaufman, 1969), and the National Bureau of Standards (NBS, 1952).

Energies for levels that have not been previously measured can be calculated using the Rydberg formula, equation (1). A least squares fit is used to determine the slope, α , in equation (2), of the quantum defect versus energy plot for the candidate series.

Complete assignment of the observed series is not always possible based on knowledge of the energy levels. This is because the error in the measurements is larger than the fine structure splitting. Under these circumstances, assignment is made based upon the intensities of the observed lines and the relative intensities predicted by the selection rules and the results of Faust and McFarlane presented in Tables I and II.

V. Results and Discussion

Observations

The spectral scan permitted observation of thirty transitions. Terms belonging to the seven series identified are 9p[1/2]1, 9-13p[5/2]3, 9-13p[3/2]2, 7-10f[3/2]2, 7-10f[5/2]3, 9-10p'[1/2]1, 9-11p'[3/2]1, and 4f'[5/2]2. All observed transitions were allowed according to selection rules except for that one corresponding to the 4f'[5/2]2 level. Figure 7 is a partial energy level diagram of krypton illustrating which transitions were observed.

Energy Levels and Recorded Spectra

Based on the rationale for series identification discussed in the last chapter, the measured transition energies of the lines and calculated values for the quantum defect, u, and effective quantum number, n^* , are given in Tables III-IX. Values for known or calculated transition energies are also included. The known energies used in identifying the lines were determined by Moore of the NBS (NBS, 1952). A correction factor of $-0.76\ cm^{-1}$ has been used to adjust these values (Tanaka and Yoshino, 1979:163). Figures 8-11 are reproductions of portions of the recorded spectra.

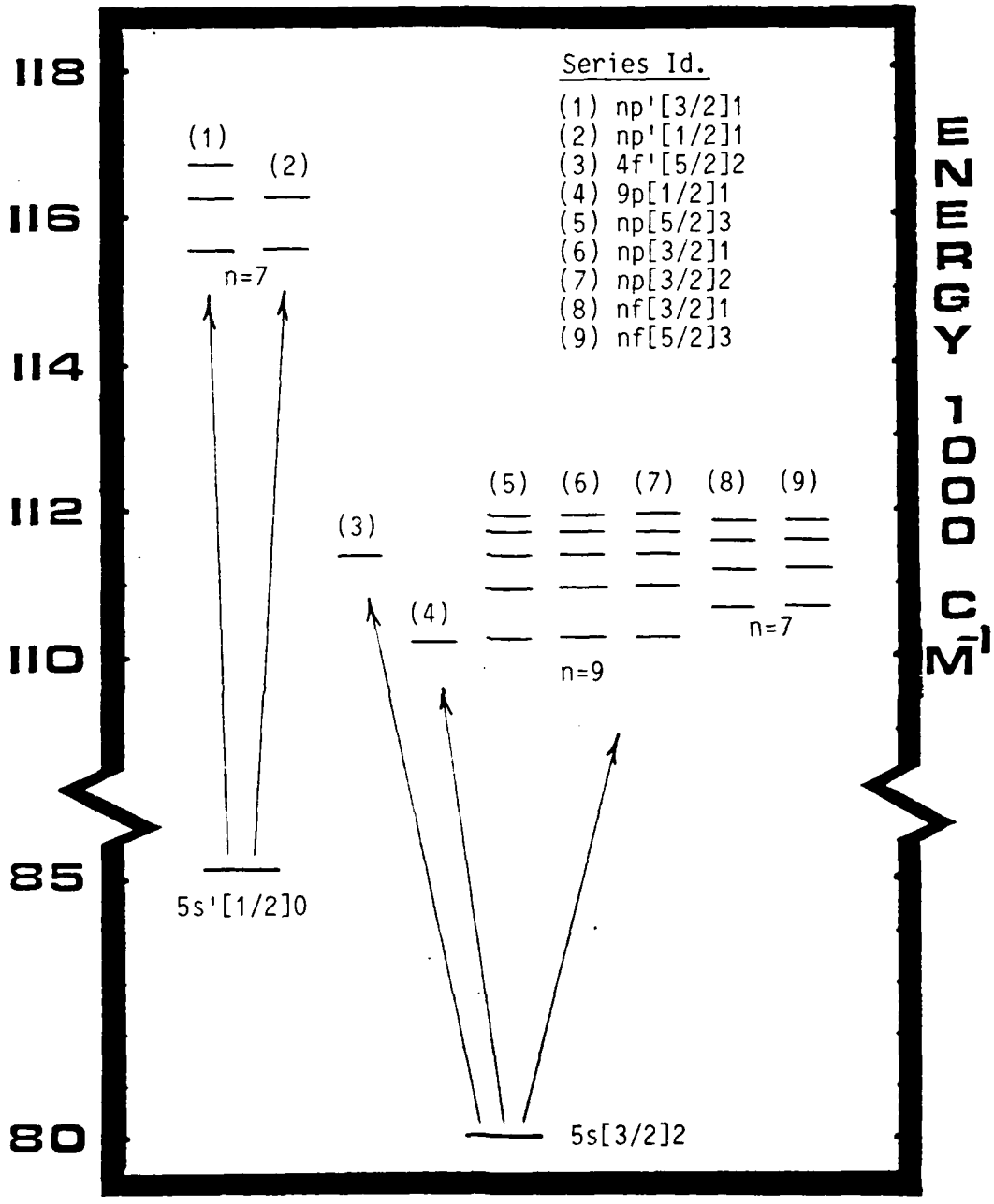

Figure 7. Krypton Energy Diagram for Observed Transitions

np[1/2]1

n	Energy (cm^{-1})	u	n*
9	30208.0	2.6653	6.3347

Measured Data

n	Energy (cm^{-1})	u	n*
9	30208.31 (K)	2.6650	6.3350

Known Data

Table III. Kr Transition Energies for np[1/2]1 Series from 5s[3/2]2 Metastable Level

np[5/2]3

n	Energy (cm^{-1})	u	n*
9	30237.9	2.6304	6.3696
10	30925.8	2.6246	7.3754
11	31378.4	2.6243	8.3757
12	31694.6	2.6232	9.3768
13	31923.2	2.6250	10.3750

Measured Data

n	Energy (cm^{-1})	u	n*
9	30237.79 (K)	2.6306	6.3695
10	30923.9 (C)	2.6272	7.3728
11	31377.9	2.6257	8.3743
12	31694.2	2.6247	9.3753
13	31923.4	2.6240	10.3760

Known and Calculated Data

Table IV. Kr Transition Energies for np[5/2]3 Series from 5s[3/2]2 Metastable Level

np[3/2]1

n	Energy (cm^{-1})	u	n*
9	30264.0	2.5995	6.4005
10	30941.8	2.5943	7.4057
11	31390.0	2.5931	8.4069
12	31701.3	2.5979	9.4021
13	31928.6	2.5974	10.4036

Measured Data

n	Energy (cm^{-1})	u	n*
9	30263.08 (K)	2.6006	6.3994
10	30940.5 (C)	2.5967	7.4033
11	31389.2	2.5953	8.4047
12	31702.3	2.5941	9.4059
13	31929.4	2.5933	10.4067

Known and Calculated Data

Table V. Kr Transition Energies for np[3/2]1 Series from 5s[3/2]2 Metastable Level

np[3/2]2

n	Energy (cm^{-1})	u	n*
9	30271.5	2.5905	6.4095
10	30946.8	2.5850	7.4150
11	31393.5	2.5836	8.4164
12	31704.1	2.5873	9.4127
13	31930.7	2.5866	10.4134

Measured Data

n	Energy (cm^{-1})	u	n*
9	30271.06 (K)	2.5910	6.4090
10	30944.3 (K)	2.5897	7.4103
11	31392.3 (C)	2.5869	8.4131
12	31704.5	2.5858	9.4143
13	31931.0	2.5851	10.4149

Known and Calculated Data

Table VI. Kr Transition Energies for np[3/2]2 Series from 5s[3/2]2 Metastable Level

nf[3/2]2

n	Energy (cm^{-1})	u	n*
7	30684.3	0.02927	6.97073
8	31214.9	0.03047	7.96953
9	31578.6	0.03072	8.96928
10	31838.4	0.03131	9.96869

Measured Data

n	Energy (cm^{-1})	u	n*
7	30684.24 (K)	0.02936	6.97064
8	31215.1 (C)	0.03001	7.97000
9	31578.7	0.03039	8.96961
10	31838.6	0.03040	9.96960

Known and Calculated Data

Table VII. Kr Transition Energies for nf[3/2]2 Series from 5s[3/2]2 Metastable Level

nf[5/2]3

n	Energy (cm^{-1})	u	n*
7	30694.0	0.01425	6.98575
8	31220.9	0.01659	7.98341
9	31583.9	0.01324	8.98676
10	31842.4	0.01320	9.98680

Measured Data

n	Energy (cm^{-1})	u	n*
7	30693.68 (K)	0.01475	6.98525
8	31220.89	0.01661	7.98339
9	31584.00	0.01291	8.98709
10	31841.64	0.01665	9.98335

Known Data

Table VIII. Kr Transition Energies for nf[5/2]3 Series from 5s[3/2]2 Metastable Level

np'[3/2]1

n	Energy (cm^{-1})	u	n*
9	30383.7	2.6356	6.3644
10	31071.4	2.6322	7.3673
11	31525.0	2.6337	8.3662

Measured Data

n	Energy (cm^{-1})	u	n*
9	30381.4 (C)	2.6383	6.3617
10	31069.3	2.6360	7.3634
11	31524.8	2.6346	8.3654

Calculated Data

Table IX. Kr Transition Energies for np'[3/2]1 Series from 5s'[1/2]0 Metastable Level

np'[1/2]1

n	Energy (cm^{-1})	u	n*
9	30395.1	2.6222	6.3778
10	31078.8	2.6187	7.3813

Measured Data

n	Energy (cm^{-1})	u	n*
9	30389.7 (C)	2.6286	6.3714
10	31074.4	2.6267	7.3733

Calculated Data

Table X. Kr Transition Energies for np'[1/2]1 Series from 5s'[1/2]0 Metastable Level

$np'[5/2]2$

n	Energy (cm^{-1})	u	n*
4	31410.1	0.01282	3.98718

Measured Data

n	Energy (cm^{-1})	u	n*
4	31409.42 (K)	0.01301	3.98699

Known Data

Table XI. Kr Transition Energies for $nf'[5/2]2$ Series from $5s[3/2]2$ Metastable Level

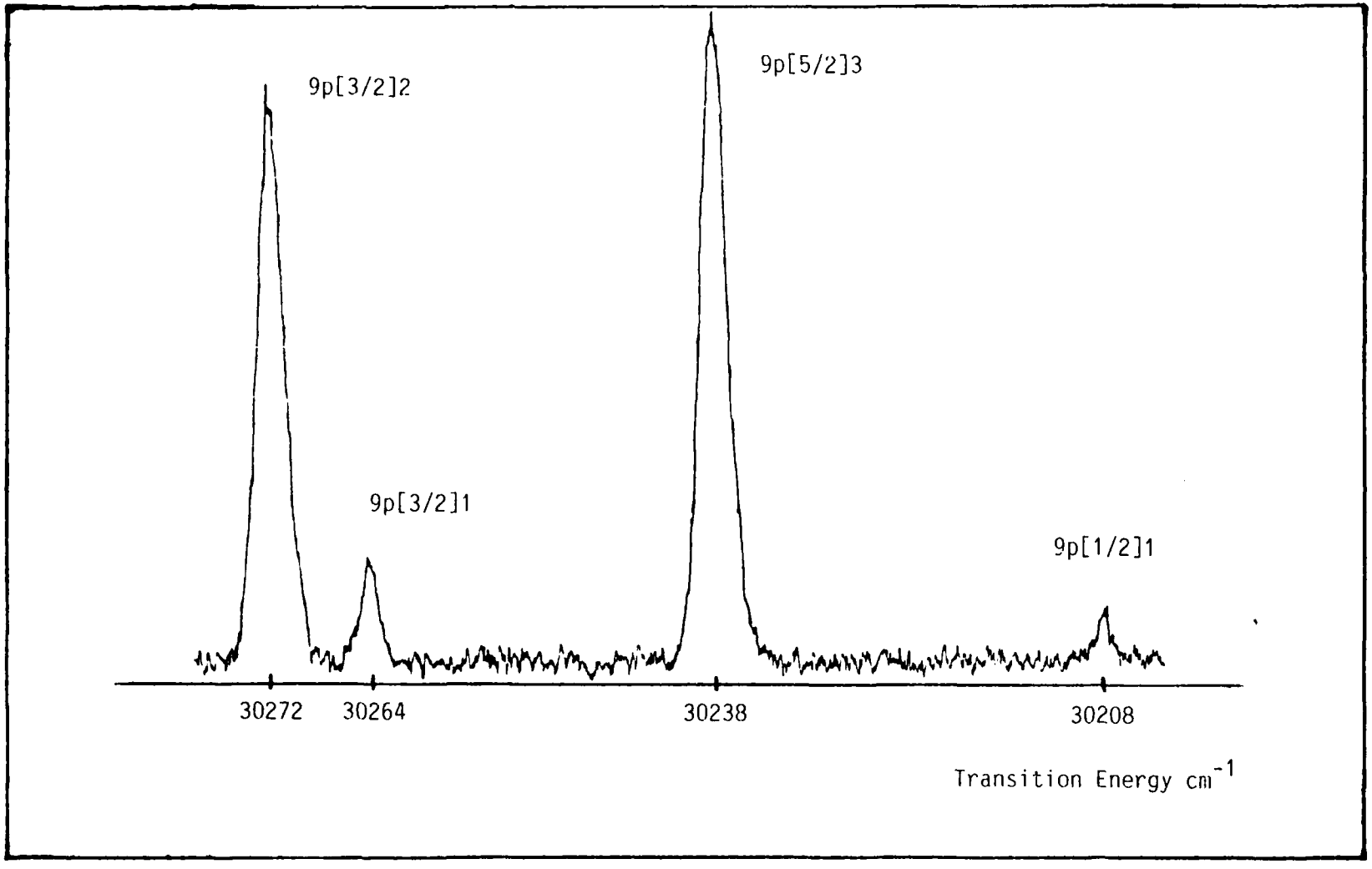

Figure 8. Recorded Kr Spectra of the 9p[3/2]2, 9p[3/2]1, 9p[5/2]3, and 9p[1/2]1 Series Terms

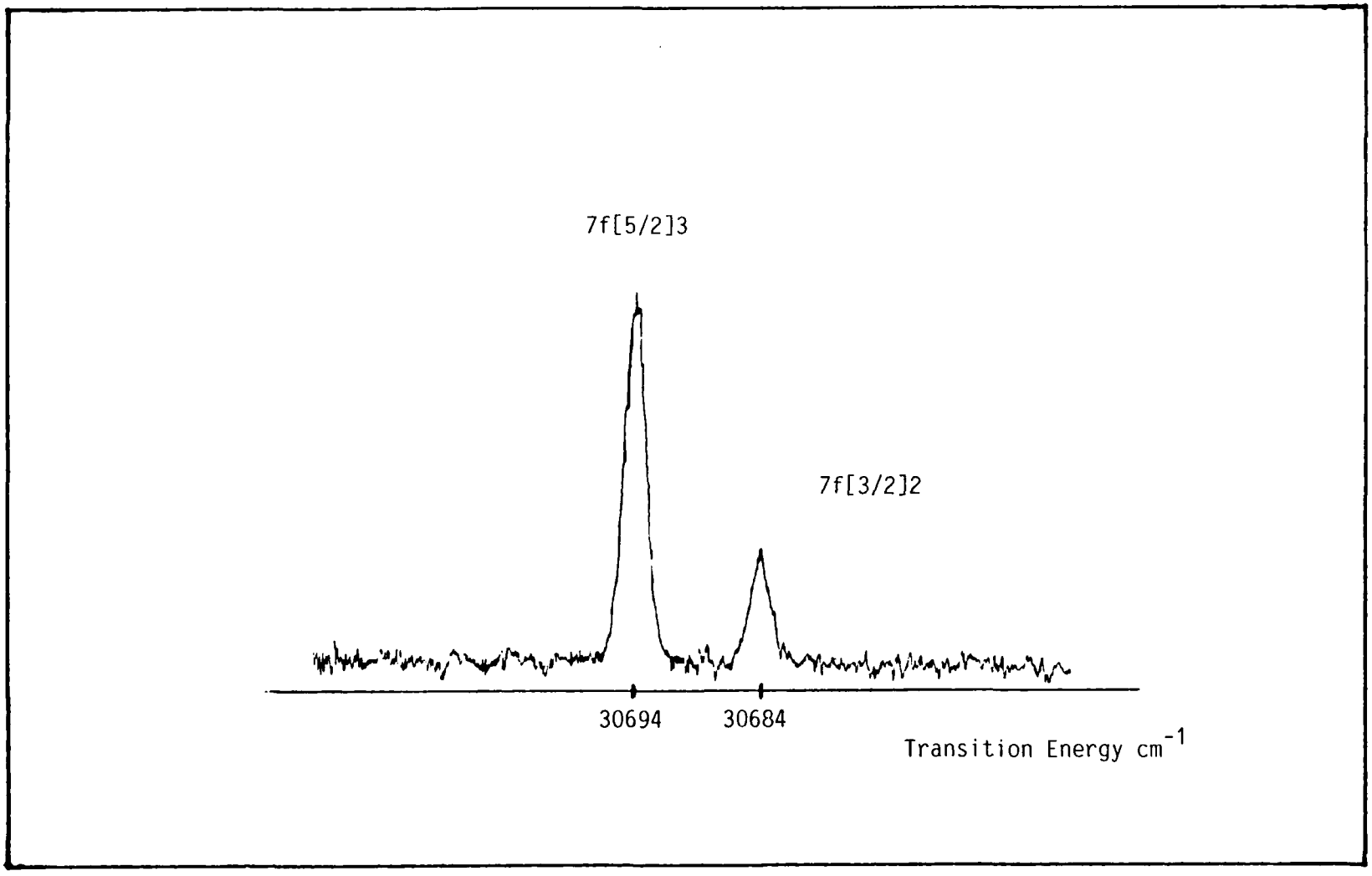

Figure 9. Recorded Kr Spectra of the 7f[3/2]2 and 7f[5/2]3 Series Terms

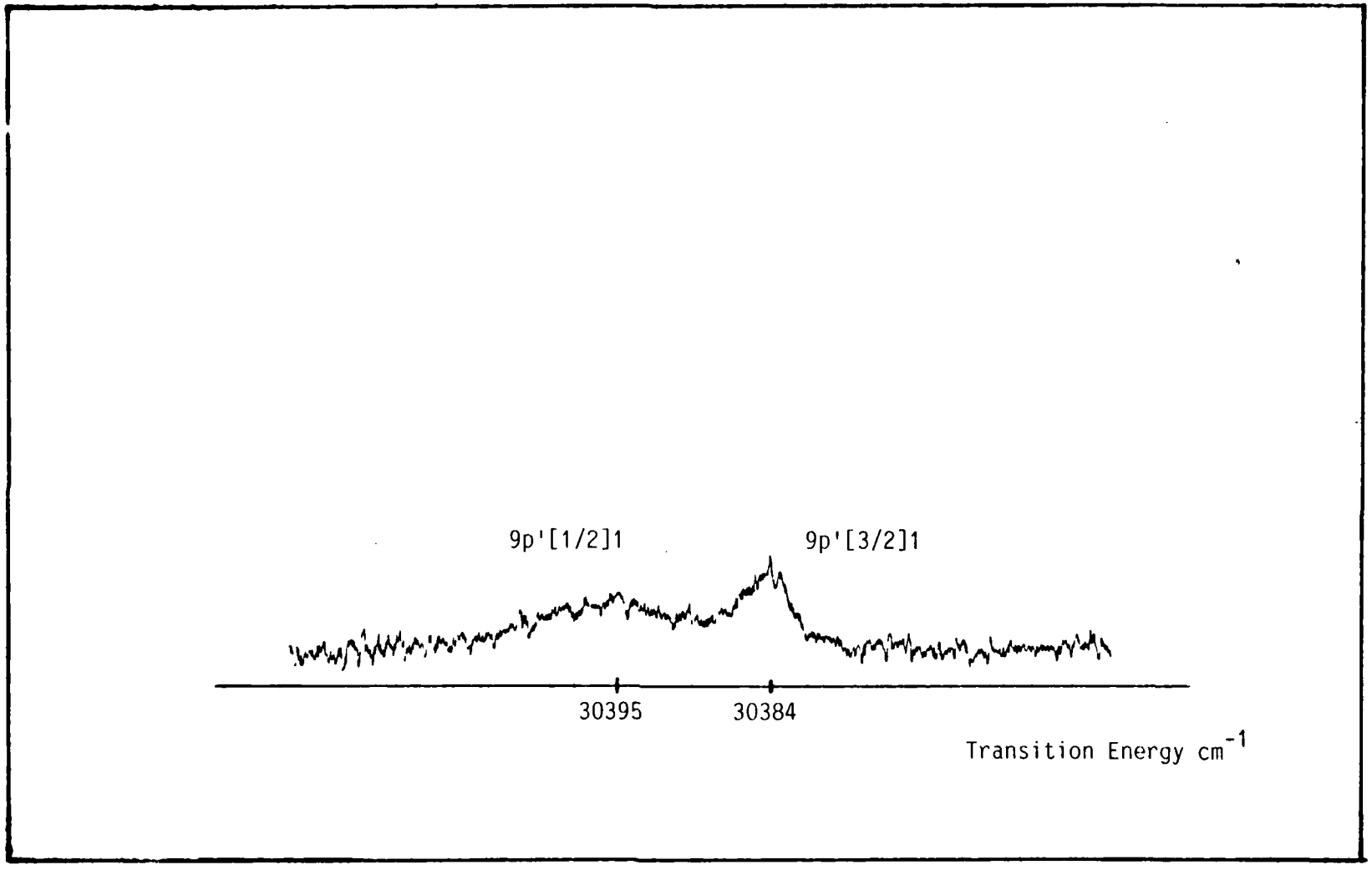

Figure 10. Recorded Kr Spectra of the 9p'[3/2]1 and 9p'[1/2]1 Series Terms

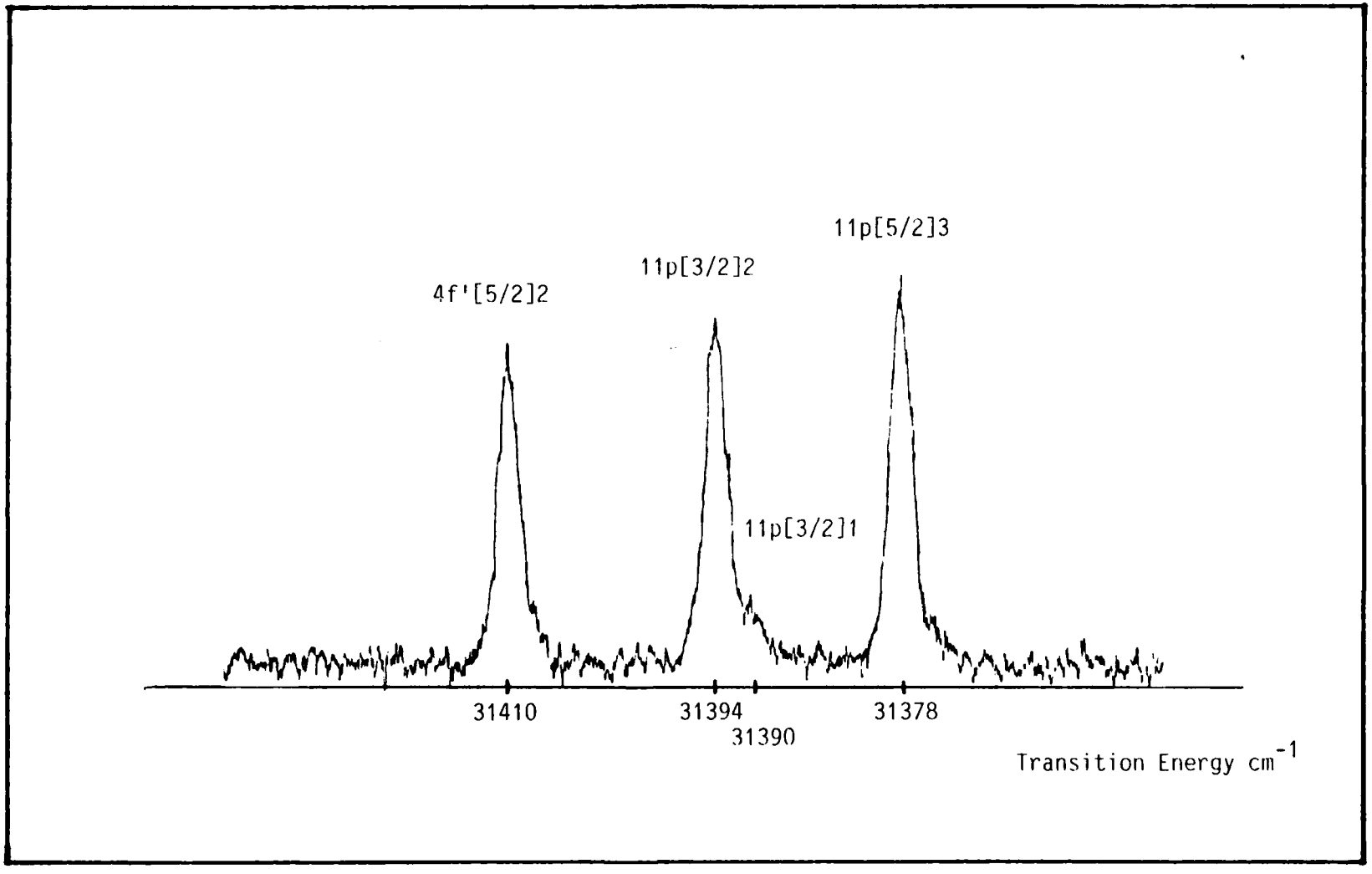

Figure 11. Recorded Kr Spectra of the 4f'[5/2]2, 11p[3/2]2, 11p[3/2]1, and 11p[5/2]3 Series Terms

Comparison With Known Data

Comparing the energy levels just obtained to known data led to an initial identification of fourteen lines belonging to seven different series. Five of the lines could be exactly specified. These lines correspond to the terms 9p[1/2]1, 9p[3/2]2 and 10p[3/2]2, 9p[3/2]1, and 4f'[5/2]2 . The resolution of the remaining data prohibited assignment of the proper J values because the fine structure separation was less than the accuracy of the measurements, 0.9 cm^{-1} . Five members of the series identified as np[3/2]1 and np[3/2]2 were resolvable in the recorded data. The 9p[1/2]1 and 4f'[5/2]2 terms appeared only once over the range of the scan. The rest of the fourteen lines were tentatively assigned as belonging to the following terms: 9-13p[5/2]J=2 or 3 , 7-10f[3/2]J=1 or 2 , and 7-10f[5/2]J=2 or 3 . All of these terms originated from the 5s[3/2]2 metastable level.

Comparison With Calculated Data

Energy levels for the apparent series identified above as np[5/2]J, np[3/2]1 , and np[3/2]2 were calculated using the Rydberg formula, equation (1), as mentioned in the previous chapter. The calculated energies agree quite well with the measured data. A maximum deviation of 1.4 cm^{-1} is observed for the 10p[5/2]J term.

Analyses of the remaining two series were made considering all possible allowed transitions from the 5s[3/2]2 metastable level with no successful results. Transitions from the 5s'[1/2]0 level were then considered. The only allowed transitions from this level are to the

even parity levels for which K = 1/2 or 3/2 and J = 1 since K cannot be negative and the J = 0 to 0 transition is forbidden. The intensity ratio for the two lines is approximately 2:1 which is the same as that indicated in Table II for s'[1/2]0 to p'[3/2]1 and p'[1/2]1 transitions. Thus, the np'[3/2]1 and np'[1/2]1 levels were considered first.

Comparison of the calculated values with the measured data agrees reasonably well considering that only two data points exist from which to determine the slope of the quantum defect versus energy plot. The maximum difference in energy was 2.3 and 5.4 cm^{-1} for the 9p'[3/2]1 and 9p'[1/2]1 terms, respectively.

Relative Line Intensities

Assignment of a specific J value to the series np[5/2]J=2 or 3 , nf[3/2]J=1 or 2 , and nf[5/2]J=2 or 3 was necessary to completely specify the rest of the observed lines. This assignment was made based upon the intensities of the observed lines and the relative intensities predicted be selection rules and the results of Faust and McFarlane presented in Table I. The intensity ratios for the np[3/2]2 to np[3/2]1 , and the np'[3/2]1 to np'[1/2]1 lines are 10:1 and 2:1, respectively. This is a good agreement with those provided in Tables I and II which are 9:1 and 2:1.

The predicted relative intensities for the np[5/2]3 to np[5/2]2 lines are given in Table I as 14:1. Consequently, the line originally identified as np[5/2]J was assigned a J value of 3. In making this assignment, there was a small disagreement between observed and predicted relative intensities for the np[5/2]3 to np[3/2]2 lines. The observed intensity ratio is approximately 1.1:1 as compared to the predicted 1.6:1. This result was much easier to accept than that obtained if a J value of 2 was assigned to the line. That would make the predicted intensity rato 1:9 which would have been unacceptable.

An interesting feature which appeared once during the scan adds a degree of confidence to the J = 3 assignment. This is shown in Figure 11. The p series lines illustrated all have principal quantum numbers of n = 11. A small line is observed on the long wavelength side of what has been identified as the 11p[5/2]3 term. The intensity ratio for these two lines is approximately 14:1, exactly that which is predicted by Faust and McFarlane. The calculated energy for the 11p[5/2]2 line, however, indicates that it should appear on the short wavelength side of the 11p[5/2]3 term as it does for lower values of n. Some perturbation appears to be in effect.

The J values for the nf[3/2]J and nf[5/2]J were assigned as being equal to 1 and 3, respectively. This assignment was based upon fairly good agreement of the intensity relations observed for the other lines which indicated that equal changes of J and K in the same direction yield the strongest lines.

The Forbidden Transition

The only observed forbidden transition, as was mentioned earlier, was that from the 5s[3/2]2 metastable to the 4f'[5/2]2. (The reason for selecting the J=2 term was because of the 1.56 cm^{-1} energy difference between measured and known levels for J=3.) This required a unit change in the value of the angular momentum of the atom core from 3/2 to 1/2. A similar forbidden transition was observed in xenon (Cook and others, 1975:1455) where transitions from the mestastable 6s'[1/2]0 to the np[1/2]1 and np[3/2]1 levels occurred. The hypothesis resulting from this work was that although j-1 coupling may be more appropriate than either L-S or j-j coupling, it was still by no means entirely satisfactory. An additional observation concerning both the krypton transition of this work and the cited forbidden transition in xenon was that intensity rules were not obeyed. Recall that rather good agreement had been observed when determining the J values of the observed lines for the allowed transitions. In those instances, a change of J and K in the same direction produced the strongest lines. In the present case, K increases by one while J remains unchanged. Yet, the intensity of the line in Figure 11 is relatively strong. The intensity rules would predict that the 4f'[5/2]3 line would be stronger if they were valid for transitions involving changes in the core momentum. This does not appear to be the case.

Error Analysis

The accuracy of the measurements based on the resolution of both the neon calibration lines and the krypton spectra alone is 0.9 cm^{-1}. Several measurements fall outside of this tolerance when compared with

known or calculated values. However, these deviations can be accounted for. First of all, the accuracy of the calculated values depends on the number of data points used for determination of the slope, α , in equation (2), and also on whether or not those levels were perturbed. The largest deviations occur for the np'[1/2]1 and np'[3/2]1 series, in that order. The reason for this is that the calculated values for these levels have been extrapolated using only two data points. In addition, the perturbation interaction between p and p' levels for J=1 is reportedly large for the np'[1/2]1 levels (Dunning and Stebbings, 1974:2380).

The effect of this interaction is also noticed in the levels for the np[3/2]1 series even though five data points were used in the extrapolation of quantum defects for the higher levels. The only other levels which need to be mentioned are the terms 10p[5/2]3 , 10p[3/2]1, and 10p[3/2]2 which all fall outside the 0.9 cm^{-1} accuracy figure. The cause of this error is due to the large separation of the neon calibration lines on either side of this group of 10p[K]J levels. In all other cases, the separation between calibration lines is typically 40 angstroms. The krypton lines in question fall approximately midway between the 6506 and 6402 angstrom lines, the separation of which is 104 angstroms. For the case of the neon lines with the least separation, a scale difference of 0.02 cm^{-1}/division is observed between adjacent regions. If this scale factor fluctuation can occur in a range of 40 angstroms, a similar fluctuation is likely to occur in a range of 100

angstroms. Taking into account this fluctuation in scaling factor, a recalculation of the energy of the 10p[3/2]2 level yields an energy difference of approximately 0.94 cm^{-1} from the known value.

VI. Conclusions and Recommendations

Conclusions

Of the thirty term values measured, nineteen had not been previously observed. In almost all cases, the accuracy obtained was 0.9 cm^{-1} .

For the experimental equipment used, it was found that a random error of + 0.02 cm^{-1} per division in the scaling factor existed over a range of approximately 50 angstroms in the neon scan. This error can be attributed to small variations in the speed of the scan and of the chart recorder.

The error of the energies calculated with the Rydberg formula were in almost all cases less than 1 cm^{-1} . Three or more data points were necessary to extrapolate values for quantum defects at higher energies to achieve this accuracy.

Another factor limiting resolution for the higher energy levels was the signal-to-noise ratio. Laser power was limited to that used to prevent damage to the crystal of the SHG Autotracker. Consequently, the discharge tube noise prohibited resolution of the fine spectra structure.

Recommendations

The identification of several series observed was based upon intensities of the transitions when the fine structure could not be resolved. Confirmation of the assignments can be made by observation of the lower order terms where the fine structure splitting is larger. For example, the splitting of the 6p[5/2]J level is approximately 5 cm^{-1}.

Relative intensities of the lower order terms could be correlated with those predicted by tne intensity rules.

User of Rhodamine 610 or 640 dye will allow scanning through wavelengths capable of reaching the first ionisation limit at maximum laser power. Because of the rapid drop of signal intensity with increasing principal quantum number, however, the noise level of the tube will again be the limiting factor.

An analysis of the discharge tube noise characteristics for various pressures, discharge currents, and gas mixtures would provide a much higher degree of confidence that a minimal noise level was actually achieved. Different electrode and tube geometries could also be considered.

Appendix A

Equipment List

Item	Manufacturer	Model
a. Nd:Yag Laser	Quanta-Ray	DCR-2A-10
b. Power Supply	Quanta-Ray	DCR-2A-10
c. Second Harmonic Generator SHG II	Quanta-Ray	HG-2
d. Temperature Controller	Quanta-Ray	HG-2
e. Pulsed Dye Laser	Quanta-Ray	PDL-1
f. Dye Laser Controller	Quanta-Ray	MCI-1
g. Dye Pump	Quanta-Ray	TSC-1
h. SHG Autotracker	Inrad	5-12
i. KDP-C Crystal	Inrad	none
j. Servo Driver	Inrad	5-12
k. Oscilloscope	Tektronix	7904
l. Programmable Digitizer	Tektronix	7D20
m. DC Power Supply	Hewlett-Packard	HP6234A
n. DC Power Supply	Hewlett-Packard	HP6525A
o. Boxcar Integrator	Princeton Applied Research	160
p. Bandpass Amplifier	Princeton Applied Research	113
q. Chart Recorder	Hewlett-Packard	7132A
r. Discharge Tube	Mr. J. Ray Power Propulsion WP-AFB, OH	

Equipment List (Continued)

Item	Manufacturer	Model
s. Neon Calibration Lamp	Unknown	
t. Laser Dye	Exciton	DCM
u. Assorted Optics Elements		
v. Assorted Electrical Components		

Bibliography

Biraben, F. and others. "Optogalvanic Spectroscopy of the ns and nd Rydberg States of Xenon," Journal of Physics (B), 15: 2595-2603 (1982).

Cook, T.B. and others. "Studies of Xenon Atoms in High Rydberg States," Physical Review (A), 12: 1453-1458 (1975).

Delsart, C., Keller, J.C. and C. Thomas. "Laser Investigation of Odd Krypton Rydberg Levels Using the Field Ionisation Detection Method," Journal of Physics (B), 14: 4241-4254 (1981).

Delsart, C., Keller, J.C. and C. Thomas. "Optogalvanic Detection of Krypton Rydberg Levels with a Two-Step Pulsed Laser Excitation," Journal of Physics (B), 14: 3355-3361 (1981).

Dunning, F.B. and R.F. Stebbings. "Role of Autoionization in the Near-Threshold Photoionization of Argon and Krypton Metastable Atoms," Physical Review (A), 9: 2378-2382 (1974).

Faust, W.L. and R.A. McFarlane. "Line Strengths for Noble-Gas Maser Transitions; Calculations of Gain/Inversion at Various Wavelengths," Journal of Applied Physics, 35: 2010-2015 (1964).

Fried, Bernard and George Shortley. "Structure of the Configurations of High Azimuthal Quantum Number in Cu II and the Rare Gases," Physical Review, 54: 749-753 (1938).

Green, R.B. and others. "Galvanic Detection of Optical Absorptions in a Gas Discharge," Applied Physics Letters, 29: 727-729 (1976).

Herzberg, Gerhard. Atomic Spectra and Atomic Structure. New York: Prentice-Hall Inc., 1937.

Humphreys, C.J. and V. Kaufman. "Accurate Energy Levels and Calculated Wavelengths of Kr I," Journal of the Optical Society of America, 59: 1614-1628 (1969).

King, David S. and Peter K. Schenck. "Optogalvanic Spectroscopy," Laser Focus, 50-57 (March 1978).

Koster, G.F. and H. Statz. "Probabilities for the Neon Laser Transitions," Journal of Applied Physics, 32: 2054-2055 (1961).

Meissner, K.W. and W.F. Miller. "Influence of Irradiation on the Characteristic of a Glow Discharge in the Rare Gases," Physical Review, 92: 896-898 (1953).

National Bureau of Standards. Atomic Energy Levels as Derived from the Analysis of Optical Spectra. Circular 467, Vol. 2. Washington: U.S. Government Printing Office, 1952.

Racah, G. "On a New Type of Vector Coupling in Complex Spectra," Physical Review, 61: 537 (1942).

Tanaka, Y. and K. Yoshino. "Absorption Spectrum of Krypton in the Vacuum UV Region," Journal of the Optical Society of America, 69: 159-165 (1979).

White, Harvey E. Introduction to Atomic Spectra. New York: McGraw-Hill Book Co., 1934.

VITA

First Lieutenant Mikal S. Kandola was born on 21 July 1959 in Barre, Vermont. He graduated from Silver Lake Regional High School in Kingston, Massachusetts in 1977 and attended Norwich University in Northfield, Vermont from which he received the Bachelor of Science in Electrical Engineering in May 1981.

Upon graduation, he received a commission in the USAF through the ROTC program. He was stationed at Headquarters Electronic Systems Division, Hanscom AFB in Bedford, Massachusetts where he served as electrical engineer for the Strategic Communications Systems Directorate until entering the School of Engineering, Air Force Institute of Technology, in June 1983.

Permanent address: 26 Riverside Drive
Kingston, Massachusetts 02364

UNCLASSIFIED

SECURITY CLASSIFICATION OF THIS PAGE

REPORT DOCUMENTATION PAGE

1a REPORT SECURITY CLASSIFICATION UNCLASSIFIED	1b. RESTRICTIVE MARKINGS
2a SECURITY CLASSIFICATION AUTHORITY	3. DISTRIBUTION/AVAILABILITY OF REPORT Approved for public release; distribution unlimited.
2b DECLASSIFICATION/DOWNGRADING SCHEDULE	
4 PERFORMING ORGANIZATION REPORT NUMBER(S) AFIT/GEO/PH/84D-2	5. MONITORING ORGANIZATION REPORT NUMBER(S)
6a NAME OF PERFORMING ORGANIZATION School of Engineering 6b. OFFICE SYMBOL (If applicable) AFIT/ENP	7a. NAME OF MONITORING ORGANIZATION
6c. ADDRESS (City, State and ZIP Code) Air Force Institute of Technology Wright-Patterson AFB, Ohio 45433	7b. ADDRESS (City, State and ZIP Code)
8a NAME OF FUNDING/SPONSORING ORGANIZATION Power Propulsion Lab 8b. OFFICE SYMBOL (If applicable) AFWAL/POOC	9. PROCUREMENT INSTRUMENT IDENTIFICATION NUMBER
8c ADDRESS (City, State and ZIP Code) Air Force Wright Aeronautical Lab Wright-Patterson AFB, Ohio 45433	10. SOURCE OF FUNDING NOS. PROGRAM ELEMENT NO / PROJECT NO. / TASK NO. / WORK UNIT NO.
11 TITLE (Include Security Classification) See box 19	
12 PERSONAL AUTHOR(S) Mikal S. Kandola, B.S., 1st Lt, USAF	
13a TYPE OF REPORT MS Thesis 13b. TIME COVERED FROM _____ TO _____	14 DATE OF REPORT (Yr., Mo., Day) 1984 December 15. PAGE COUNT 57
16. SUPPLEMENTARY NOTATION	

17 COSATI CODES		
FIELD	GROUP	SUB GR
07	04	
20	06	

18 SUBJECT TERMS (Continue on reverse if necessary and identify by block number)
Krypton, Rydberg atoms, atomic spectra, optogalvanic spectroscopy.

19 ABSTRACT (Continue on reverse if necessary and identify by block number)

Title: OPTOGALVANIC MEASUREMENT OF EVEN PARITY RYDBERG LEVELS IN KRYPTON GAS

Thesis Chairman: Won B. Roh, PhD
Associate Professor of Physics

Approved for public release: IAW AFR 190-17.
21 Feb 85
LYNN E. WOLAVER
Dean for Research and Professional Development
AFIT/NR

20 DISTRIBUTION/AVAILABILITY OF ABSTRACT UNCLASSIFIED/UNLIMITED ☒ SAME AS RPT ☐ DTIC USERS ☐	21 ABSTRACT SECURITY CLASSIFICATION UNCLASSIFIED
22a NAME OF RESPONSIBLE INDIVIDUAL Mikal S. Kandola, 1st Lt, USAF	22b TELEPHONE NUMBER (Include Area Code) (513) 255-5533 22c OFFICE SYMBOL AFIT/ENP

DD FORM 1473, 83 APR EDITION OF 1 JAN 73 IS OBSOLETE

UNCLASSIFIED

SECURITY CLASSIFICATION OF THIS PAGE

An optogalvanic detection scheme, in conjunction with a single-step pulsed laser excitation has been used to measure the energy of even parity Rydberg levels in krypton. The excitation scheme starts from the 5s[3/2]2 and 5s'[1/2]0 metastable states, which have been populated in a He-Kr discharge tube.

Members belonging to the even parity series np[1/2]1, np[5/2]3, np[3/2]1, np[3/2]2, nf[5/2]3, nf[3/2]2, np'[3/2]1, and np'[1/2]1 have been observed and their energies measured with an accuracy of 0.9 cm^{-1}. The 4f'[5/2]2 term was also observed and it has been found to originate from the 5s[3/2]2 metastable level, in violation of selection rules.

Measured energies were compared to either calculated or previously measured values. Calculated energies were obtained with the Rydberg formula using quantum defects extrapolated from the known low-lying levels.

END

FILMED

5-85

DTIC